



ELSEVIER

Contents lists available at ScienceDirect

Physica D

journal homepage: [www.elsevier.com/locate/physd](http://www.elsevier.com/locate/physd)

# Friction factor correlations for laminar, transition and turbulent flow in smooth pipes

Daniel D. Joseph<sup>a,b,\*</sup>, Bobby H. Yang<sup>a,c</sup>

<sup>a</sup> Department of Aerospace Engineering and Mechanics, University of Minnesota, MN 55455, USA

<sup>b</sup> Department of Mechanical and Aerospace Engineering, University of California - Irvine, CA 92617, USA

<sup>c</sup> CIMAS, Rosenstiel School of Marine and Atmospheric Science, University of Miami, FL 33149, USA

## ARTICLE INFO

### Article history:

Available online xxxx

## ABSTRACT

In this paper we derive an accurate composite friction factor vs. Reynolds number correlation formula for laminar, transition and turbulent flow in smooth pipes. The correlation is given as a rational fraction of rational fractions of power laws which is systematically generated by smoothly connecting linear splines in log–log coordinates with a logistic dose curve algorithm. This kind of correlation seeks the most accurate representation of the data independent of any input from theories arising from the researchers' ideas about the underlying fluid mechanics. As such, these correlations provide an objective metric against which observations and other theoretical correlations may be applied. Our correlation is as accurate, or more accurate, than other correlations in the range of Reynolds numbers in which the correlations overlap. However, our formula is not restricted to certain ranges of Reynolds numbers but instead applies uniformly to all smooth pipe flow data for which data is available. The properties of the classical logistic dose response curve are reviewed and extended to problems described by multiple branches of power laws. This extended method of fitting which leads to rational fractions of power laws is applied to data of Marusic and Perry (1995) [15] for the velocity profile in a boundary layer on a flat plate with an adverse pressure gradient, to data of Nikuradse (1932) [3] and McKeon et al. (2004) [4] on friction factors for flow in smooth pipes and to the data of Nikuradse [1] for effectively smooth pipes.

© 2009 Elsevier B.V. All rights reserved.

Q1

## 1. Introduction

The goal of this paper is to extract analytic formulas relating the friction factor  $\lambda = -d(dp/dx) / (\rho \bar{U}^2/2)$  to the Reynolds number  $Re = \bar{U}d/\nu$  ( $\bar{U}$  being the average bulk velocity) from processing of data for flow in smooth pipes. No pipe can be perfectly smooth but when the roughness is small enough the flow depends only on the Reynolds number  $\lambda = f(Re)$  (and not on roughness) and the pipe is said to be effectively smooth.

An expanded data set for flow in smooth pipes is created by extracting results for effectively smooth pipes from data of Nikuradse [1] for flows spanning laminar, transition and turbulent flow in rough pipes. New results are obtained by direct comparison of data for smooth pipes with data for effectively smooth pipes. We also present results comparing formulas for turbulent flow in smooth pipes based on modifications of classical log laws and the formula anchored in the theory of incomplete similarity (a power law for

$\lambda = f(Re)$  with a prefactor and exponent that also depend on  $Re$ ) with each other and with the expanded data set. The principal results of this paper arise from the introduction of a new and systematic method for processing experimental data which can be described fitting data piecewise by linear splines (which are power laws in log–log coordinates). The data in the transition regions between the splines is processed by fitting five points with a logistic dose algorithm. This method of fitting leads to rational fractions of power laws and rational fractions of rational fractions of power laws. It is a fundamentally different from other methods of processing data. Other methods are motivated by flow fundamentals modulated by the researchers' imagination. Our goal is to get formulas of the highest accuracy and greatest range; ideas about fluid mechanics and turbulence do not enter at any stage. We will show that our correlation is as accurate, or more accurate, than other correlations in the range of Reynolds numbers in which the correlations overlap. However, our formula is not restricted to certain ranges of Reynolds numbers but instead applies uniformly to all smooth pipe flow data for which data is available. Other methods for describing data on turbulent flow in pipes and boundary layers are rooted in hypotheses about the controlling fluid mechanics principles under sway. It can be said that the implementation of the fluid mechanics' ideas require a certain number of operational hypotheses leading

\* Corresponding author at: Department of Aerospace Engineering and Mechanics, University of Minnesota, MN 55455, USA. Tel.: +1 612 338 4893; fax: +1 612 626 1558.

E-mail address: [joseph@aem.umn.edu](mailto:joseph@aem.umn.edu) (D.D. Joseph).

to functional forms involving unknown quantities which must finally be selected to fit the data. In this sense, all these fluid mechanics motivated fitting methods are semi-empirical. An excellent description of the most popular of these methods has appeared in the review paper of Barenblatt and Chorin [2] cited below.

During the more than 60 years of active research into turbulent pipe flow, two contrasting laws for the velocity distribution in the intermediate region have coexisted in the literature (see, eg. Schlichting 1968): the first is the power or scaling law,

$$\phi = C\eta^\alpha \quad (1.1)$$

where the  $C$  and  $\alpha$  are constants (i.e. parameters independent of  $\eta$ ) believed to depend weakly on  $Re$ . Laws such as (1.1) were in particular proposed by engineers in the early years of turbulence research. The second law found in the literature is the universal, Reynolds number independent logarithmic law,

$$\phi = (\ln \eta) / \kappa + B \quad (1.2)$$

where  $\kappa$  (von Kármán's constant) and  $B$  are assumed to be universal, i.e.  $Re$ -independent, constants.

In more recent decades, the logarithmic law (1.2) has been emphasized over the power law (1.1), sometimes even to the exclusion of the latter. The reasons have been mainly theoretical: it was not recognized that the power law has an equally valid theoretical derivation and satisfies the approximate self-consistency (overlap) condition. This theoretical bias has been allowed to obscure the fact that the experimental data unequivocally militate in favor of the power law (1.1)....

It is generally thought that the universal logarithmic law (1.2) is in satisfactory agreement with the experimental data both in pipes and in boundary layers.... However, the scaling law (1.1) has also found experimental support, provided the dependence of the quantities  $C$  and  $\alpha$  on the Reynolds number was properly taken into account. Indeed, Schlichting, following Nikuradse, showed that the experimental data agree with the scaling law over practically the whole cross-section of a pipe....

An important conclusion has been reached: The power law (1.1) and the logarithmic law (1.2) can be derived with equal rigor but from different assumptions. The universal logarithmic law is obtained from the assumption of complete similarity in both parameters  $\eta$  and  $Re$ ; physically, this assumption means that neither the molecular viscosity  $\nu$  nor the pipe diameter  $d$  influences the flow in the intermediate region. The scaling law (1.1) is obtained from an assumption of incomplete similarity in  $\eta$  and no similarity in  $Re$ ; this assumption means that the effects of both  $\nu$  and  $d$  are perceptible in the intermediate region.

## 2. Experimental data

The data we use comes from three sources: (1) the experiments on the flow of water of in smooth pipes of Nikuradse [3], (2) the experiments of Nikuradse [1] on water flow in rough pipes from which we have extracted data for "effectively smooth pipes". Fig. 1 shows how we have selected effectively smooth pipe data from the rough pipe data. Fig. 2 shows that the smooth pipe data and effectively smooth pipe data are in good agreement. The third source of data is presented in the paper by McKeon, Swanson, Zagarola, Donnelly and Smits [4] (hereafter MSZDS). Their data for the flow of gases in smooth pipes is presented graphically in Fig. 3 and in tabular form in Table 1 of MSZDS [4]. They note that

The Princeton (Zagarola and Smits (1998), [4,6] and Oregon (Swanson et al. 2002) research groups have recently examined fully developed pipe flow using very different apparatus. Compressed air is used in the Princeton "Superpipe", whereas the Oregon device uses several room temperature gases: helium, oxygen, nitrogen, carbon dioxide and sulphur hexafluoride are used for

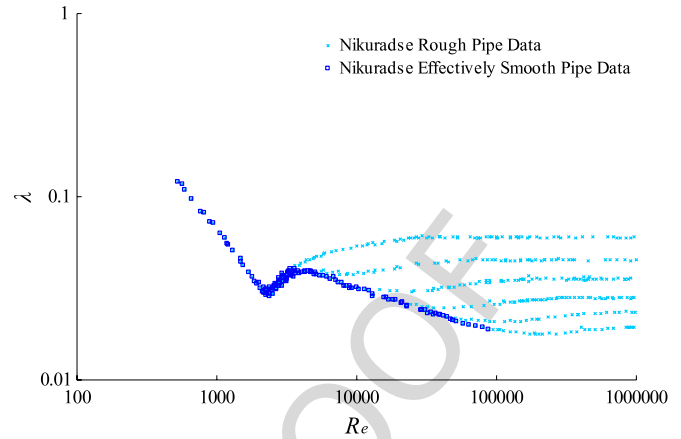


Fig. 1. Friction factor ( $\lambda$ ) vs. Reynolds number ( $Re$ ) in rough pipes [1]. The dark points on the bottom envelope of curves which depend on roughness do not depend on roughness (i.e.  $\lambda = f(Re)$ ) and can be said to be effectively smooth.

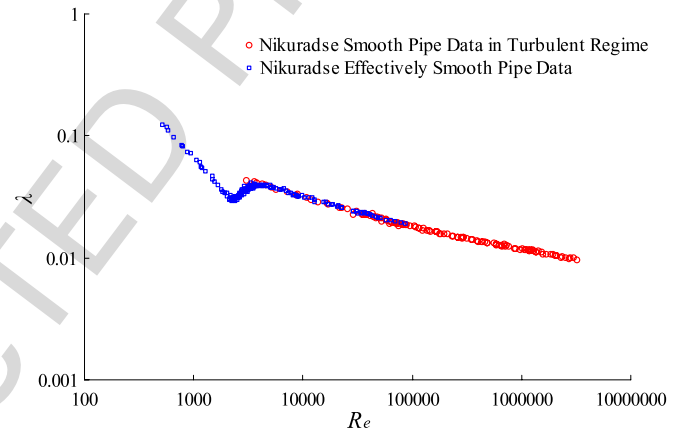


Fig. 2.  $\lambda$  vs.  $Re$  ( $3.1 \times 10^3 < Re < 3.2 \times 10^6$ ) in smooth pipes (open red circles) from [3] (open blue squares) compared with  $\lambda$  vs.  $Re$  ( $5.2 \times 10^2 < Re < 8.7 \times 10^4$ ) in effectively smooth rough pipes ([1], see Figure 1). The data for turbulent flow in effectively smooth pipes coincides with the data from smooth pipes.

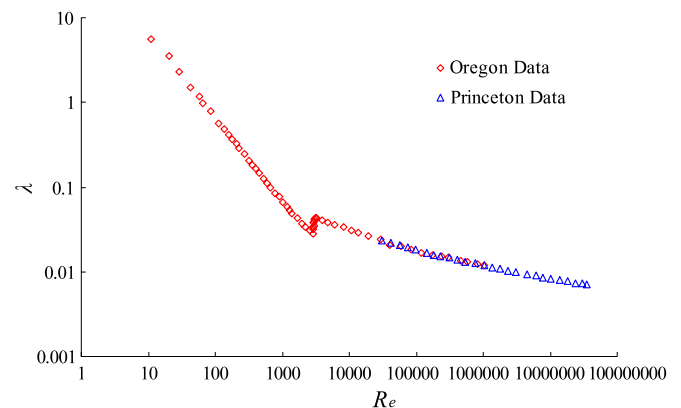
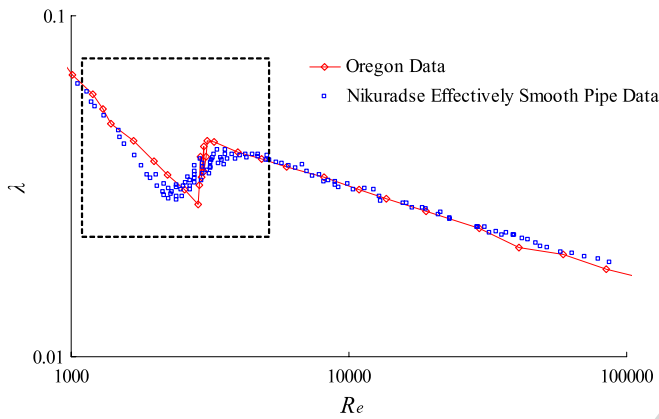


Fig. 3.  $\lambda$  vs.  $Re$  from experiments reported in MSZDS [4]. The Princeton data is in good agreement with the smooth pipe data of [3] (see Fig. 6.25 in the thesis of McKeon [5]). Fig. 4 shows that the Oregon data is not in agreement with Nikuradse's [1] data for "effectively smooth" pipes.

relatively small Reynolds numbers, and normal liquid helium (helium I) is used for highest Reynolds numbers. The difference in of the two devices is dramatic: for example, the Superpipe weighs about 25 tons, whereas the Oregon tube weighs about 1 ounce (see Fig. 4).

**Table 1**Experimental data (30 APG mean flow at  $Re = 19\,133.02$ ) for boundary layer flows with adverse pressure gradient (reproduced after Marusic and Perry [15]).

30 APG mean flow ( $Re = 19\,133.02$ )											
No.	$\phi$	$\eta$	No.	$\phi$	$\eta$	No.	$\phi$	$\eta$	No.	$\phi$	$\eta$
1	14.19779	39.48126	12	17.8959	204.6324	23	24.29825	916.1413	34	36.18715	2715.102
2	14.31916	41.87337	13	18.46791	238.6003	24	25.19049	1032.206	35	37.04935	2931.252
3	14.48314	47.04032	14	18.71844	277.0654	25	26.06025	1157.457	36	37.60313	3147.403
4	14.98265	54.50369	15	19.2299	320.1233	26	27.08825	1292.467	37	37.87272	3363.554
5	15.25863	64.45486	16	19.59897	367.9655	27	28.18673	1436.568	38	37.99084	3579.705
6	15.62833	76.89382	17	20.22202	425.7588	28	29.35161	1590.715	39	38.02275	3795.951
7	16.08429	91.91626	18	20.88928	484.0305	29	30.40133	1754.718	40	38.04359	3988.087
8	16.49045	109.4265	19	21.43574	552.0621	30	31.58338	1927.811	41	38.03168	4204.234
9	16.84369	129.4245	20	21.99511	627.6527	31	32.73956	2110.185	42	38.04827	4363.204
10	17.26571	151.8146	21	22.74916	714.0556	32	33.8983	2301.65	43	38.04868	4554.573
11	17.56293	175.7357	22	23.4404	810.1227	33	35.05426	2502.969	44	38.06908	4745.942

**Fig. 4.** Comparison of data from Nikuradse [1] for effectively smooth pipes with Oregon data (Table 1) for flow in smooth pipes. Oregon data is greatly different from Nikuradse's data in the transition region. Data in the transition is associated with the instability of laminar flow which depends on parameters like the pipe length which do not strongly influence laminar or turbulent flow. The data in the transition region forms a cloud rather than a curve.

Prior to the Princeton and Oregon experiments, the experiments performed by Nikuradse [3] covered the largest range of Reynolds numbers. Most other experiments span less than an order of magnitude in Reynolds number (see [7], Table 1.2). The data of [3,1] and MSZDS [4] is relatively easy to process and compare with empirical formulas because it is presented in tabular form.

### 3. Comparison of formulas of [8,4,6] with the data and each other

The fitting curve proposed by McKeon et al. [4] is

$$\frac{1}{\sqrt{\lambda}} = 1.930 \log \left( Re \sqrt{\lambda} \right) - 0.537; \quad (3.1)$$

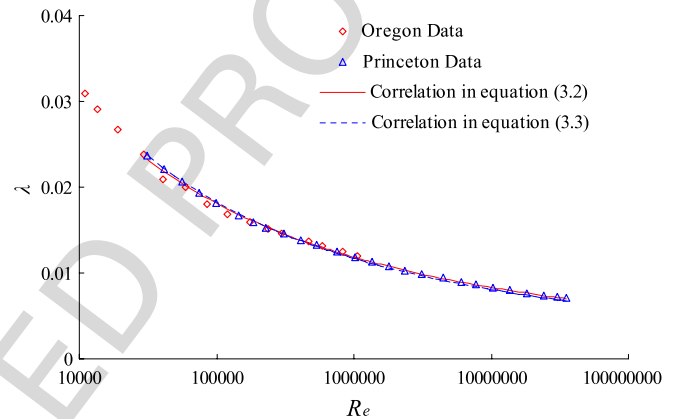
it fits Princeton data with a percentage error less than 1.25% for  $31 \times 10^3 < Re < 35 \times 10^6$  and 0.5% for  $300 \times 10^3 < Re < 13.6 \times 10^6$ .

The curve proposed by McKeon et al. [6] includes a correction for the viscous deviation from the log law at the wall and is given by

$$\frac{1}{\sqrt{\lambda}} = 1.920 \log \left( Re \sqrt{\lambda} \right) - 0.475 - \frac{7.04}{\left( Re \sqrt{\lambda} \right)^{0.55}}. \quad (3.2)$$

This equation predicts the friction factor to be within  $\pm 1.4\%$  of the Princeton data ( $\pm 0.6\%$  at high Reynolds number,  $310 \times 10^3 < Re < 30 \times 10^6$ ) and within  $\pm 2.0\%$  of the Blasius relation at low Reynolds numbers ( $10 \times 10^3 < Re < 90 \times 10^3$ ) (see Fig. 5).

Barenblatt's [8] scaling law (see Eq. (8.29) in the scaling book) is derived from an extended theory (incomplete similarity) of

**Fig. 5.** Comparison of the power law formula (3.3) and the modified log formula (3.2) with the data of MSZDS [4]. The differences between (3.2) and (3.3) are about 2% for large  $Re$  (see Fig. 10).

similarity (power law in the Reynolds number) to a form in which the prefactor and exponent of the power law also depend on the Reynolds number; the functional form of the prefactor and exponent are derived from theoretical assumptions. It is given by

$$\lambda = \frac{8}{\psi r^{2/(1+\alpha)}}, \quad (3.3)$$

$$\text{where } \psi r = \frac{e^{3/2}(\sqrt{3+5\alpha})}{2^\alpha \alpha (1+\alpha)(2+\alpha)} \text{ and } \alpha = \frac{3}{2 \ln(Re)}.$$

### 4. Logistic dose curves for data sets with multiple power law regions

Prior to the relatively recent work of Joseph and his coworkers, it was not known that the classical logistic dose response curve could be used to fit data arising from real and numerical experiments in fluid mechanics and other hard sciences. In this section we will briefly review the properties of the classical logistic dose response curve and extend this method of fitting for correlations with multiple branches of power laws. This extended method of fitting which leads to rational fractions of power laws and to rational fractions of rational fractions of power laws is applied here to data on the friction factor vs. Reynolds number for laminar, transition and turbulent flow in smooth pipes [4]; this method of fitting leads to a composite correlation which describes all the available data unrestricted by Reynolds number. The formula follows from direct processing of the data and does not depend on any assumption or correlation from fluid mechanics.

#### 4.1. Classical logistic dose response curve

The logistic function is one of the oldest growth functions and a best candidate for fitting sigmoidal (also known as "logistic")

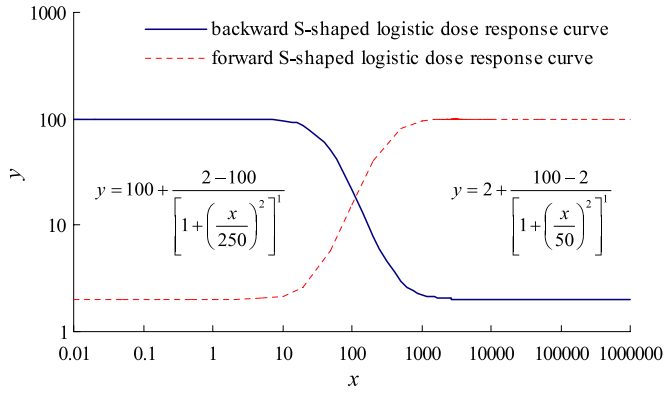


Fig. 6. Classical forward and backward logistic dose response curves.

curves. Especially the logistic dose response function is a robust fitting function for transition phenomena. The 3-parameter, 4-parameter and 5-parameter logistic dose response curves are widely used in nonlinear data fitting in life sciences; pharmacy and agronomy (see [9]).

A typical 5-parameter logistic dose response curve is given by

$$y = a + \frac{(b-a)}{\left[1 + \left(\frac{x}{t}\right)^{m \cdot n}\right]}, \quad (4.1)$$

where  $x$  and  $y$  are the independent and the dependent variables. It is widely used in the literature to describe the correlations between  $x$  and  $y$  featured by two plateau regions and a transition region. Two typical examples are shown in Fig. 6.

To our knowledge the first studies using logistic dose curve fitting in fluid mechanics can be found in the study of sedimentation by Patankar et al. [10]. This study was inspected by R. Barree who explained this method of 5-parameter fitting in an Appendix "Fitting power law data with transition regions by a continuous function: Application to the Richardson–Zaki correlation".

We shall call the correlation of data which can be described by two power laws connected by continuous data in the transition region a two power law correlation (or a bi-power law correlation). Two power law correlations for sediment transport have been studied by Wang et al. [11] and for friction factors in turbulent gas–liquid flows by Garcia et al. [12,13]. Correlations of families of bi-power laws depending on a third parameter have been constructed by Viana et al. [14] who correlated data for the rise velocity of Taylor bubbles in round vertical pipes as a family of bi-power laws of the Froude number vs. Reynolds number indexed by the Eotvos number. A file of papers correlating large data sets from real and numerical experiments can be found at (<http://www.aem.umn.edu/people/faculty/joseph/PL-correlations>).

The processing of data covered by linear splines and connected by the five-point rule of the logistic dose curve (4.1) is an approximate method whose accuracy is judged by analysis of the error of the fit. Moreover, analytical functions like (4.1) which vary on some interval cannot assume a constant value at any finite  $x$  because discontinuous derivatives are required at such points. However, functions with discontinuous derivatives can be closely modeled by analytic functions as in the case in the two logistic dose functions shown in Fig. 6. The dose function (4.1) is actually a rather complicated nonlinear function and the mathematical problem of approximation of experimental data with such functions deserves further study.

#### 4.2. Modified logistic dose response curve

The classical 5-parameter logistic dose response curve (4.1) is modeled to Eq. (4.2), in which the two constants  $a$  and  $b$  in

Eq. (4.1) are replaced by two continuous functions  $f_L(x)$  and  $f_R(x)$ , respectively.  $x_c$ ,  $m$  and  $n$  are constants.  $x_c$  is an important constant in determining the convergence trend of  $f(x)$  when the coefficient  $m$  is negative and  $n$  is a small positive number. (Hereafter  $x_c$  is called the "threshold value" of  $x$ .)

$$y = f(x) = f_L(x) + \frac{f_R(x) - f_L(x)}{G(x)} = f_L(x) + \frac{f_R(x) - f_L(x)}{\left[1 + \left(\frac{x}{x_c}\right)^m\right]^n}. \quad (4.2)$$

Here we show how to construct logistic dose curves (see Eq. (4.2)) for complicated data which can be described by piecewise continuous multiple power laws or multiple rational fractions of power laws, where the rational fractions of power laws themselves are also logistic dose functions. There are three key steps in determining a modified logistic dose curve; these are (1) the selection of two appropriate assembly members  $f_L(x)$  and  $f_R(x)$ , (2) the estimate of the threshold value  $x_c$  which identifies the point of intersection of  $f_L(x)$  and  $f_R(x)$ , and (3) the five-point sharpness control for fitting the transitional part between the two assembly members.

A main idea in the modified logistic dose curve fitting is to force the denominator function  $G(x)$  in Eq. (4.2) to move towards  $+\infty$  or 1 rapidly on different sides of the threshold value  $x_c$  once the independent variable  $x$  deviates from  $x_c$ , so that the logistic dose function can approach to  $f_L(x)$  asymptotically on one side and to  $f_R(x)$  on the other side of  $x_c$ . The two assembly members  $f_L(x)$  and  $f_R(x)$  may be constants (in this case, it will reduce to the classical logistic dose response curve), power laws, rational fractions of power laws, rational fractions of rational fractions of power laws, or any other type of continuous functions. The splitting trends of  $f(x)$  at  $x = x_c$  is the basis of the sequential construction of a rational fraction of multiple segments of power laws.

##### 4.2.1. Logistic dose curve fitting for mixed power laws and/or rational fractions of power laws

The logistic dose function for a two power law correlation (4.2) is a rational fraction of two power laws. Here we go one step further and replace one of the two member functions  $f_L(x)$  and  $f_R(x)$  in Eq. (4.2) with a rational fraction of two power laws. Then we can use the modified logistic dose curve to create a three power law correlation. If both  $f_L(x)$  and  $f_R(x)$  are replaced by rational fractions of two power laws, the modified logistic dose curve can even fit data which contains four subsections of power laws. Since  $f_L(x)$  and  $f_R(x)$  can be updated with new rational fractions again and again by adding more and more power laws, we may expect to use the modified logistic dose response curve to fit a correlation composed of five or even more branches of power laws. Such correlations lead inevitably to rational fractions of rational fractions of power laws.

##### 4.2.2. Threshold values $x_c$ of the independent variable $x$

We have found that the independent variable  $x$  is sensitive to the threshold value  $x_c$  in Eq. (4.2);  $x_c$  can be used to locate the point of intersection of the two assembly members  $f_L(x)$  and  $f_R(x)$ . That is to say,  $x = x_c$  when  $f_L(x) = f_R(x)$ . When  $x < x_c$ , the denominator function  $G(x)$  in Eq. (4.2) will approach  $+\infty$  and therefore  $f(x) \approx f_L(x)$  since  $m$  is negative. When  $x > x_c$ ,  $G(x)$  approaches to 1 asymptotically; therefore  $f(x) \approx f_R(x)$ .

##### 4.2.3. Five-point sharpness control for the transition region between $f_L(x)$ and $f_R(x)$

Data which is very close to the two assembly members  $f_L(x)$  and  $f_R(x)$  at the point  $x_c$  of intersection is said to have sharp transition. The constants  $m$  and  $n$  can control the smoothness of the transitional part between  $f_L(x)$  and  $f_R(x)$ . On the transitional part, the smoothness of data increases as the magnitude of  $m$  decreases. We use a five-point rule to judge the accuracy of the fitting

curve. Five data points on or near the transition segment of the two assembly members are selected; the errors between the five sample points and the fitting curve are calculated and evaluated by the  $R$ -square value. The goal of the five-point rule is to make the fitting curve for the five selected points as smooth as possible, which can be seen in the zoom-in view of transition region.

#### 4.2.4. Construction of a logistic dose function for data sets identified by two power laws and a smooth transition segment

In this section we illustrate the procedure for constructing a logistic dose correlation for two power laws and a smooth transition segment for data of Marusic and Perry [15] on the variation the dimensionless velocity  $\phi = u/u^*$  vs. the dimensionless distance from the wall  $\eta = u^*y/\nu$  in boundary layers with an adverse pressure gradient (APG). An example of the selection of two power laws and the calculation of sharpness control parameters  $m$  and  $n$  based on raw data is given here. The tabulated results are shown in Table 1 for 30 APG mean flow at  $Re = 19\,133.02$ .

Fig. 7 illustrates the typical procedure of the construction of a logistic dose correlation for two power laws connected by a smooth transition. Panel (a) shows all the data from Table 1. Five data segments can be identified from the graph: data segments 1, 3, 5 are three power laws segments; segments 2 and 4 are transition segments between power laws. In this example, we do not consider segments 4 and 5. Panel (b) shows two power laws  $P_1$  and  $P_2$  which are identified on segments 1 and 3, respectively. The whole plane is divided into four regions by  $P_1$  and  $P_2$  (i.e. ①, ②, ③ and ④ in panels (b) and (c)). Panel (b) clearly shows that the transition segment 2 is located in region ①. We shall show that logistic dose function of  $P_1$  and  $P_2$  cannot pass through any data points in region ①.

After  $P_1$  and  $P_2$  are determined, we can easily obtain the crossing point  $\eta = \eta_c$  by letting  $P_1 - P_2 = 0$ . The two parameters  $m$  and  $n$  are unknown, and they are obtained by substituting two data points into the following logistic function of  $P_1$  and  $P_2$ .

$$\phi = P_1(\eta) + \frac{P_2(\eta) - P_1(\eta)}{[1 + (\eta/\eta_c)^m]^n}. \quad (4.3)$$

- We tentatively choose the point A ( $\eta_1, \phi_1$ ) which is located right on the power law  $P_1$  (see panel (b) in Fig. 7). It follows that

$$\begin{aligned} \phi_1 &= P_1(\eta_1) + \frac{P_2(\eta_1) - P_1(\eta_1)}{[1 + (\eta_1/\eta_c)^m]^n} \\ &= \phi_1 + \frac{P_2(\eta_1) - \phi_1}{[1 + (\eta_1/\eta_c)^m]^n}. \end{aligned} \quad (4.4)$$

It follows that  $P_2(\eta_1) = \phi_1$  and  $P_1 = P_2$ . Only the point of intersection can satisfy this condition but it is not near the transition segment.

- Similarly, if we choose point B ( $\eta_2, \phi_2$ ) which is located on the power law  $P_2$ , we have

$$\begin{aligned} \phi_2 &= P_1(\eta_2) + \frac{P_2(\eta_2) - P_1(\eta_2)}{2[1 + (\eta_2/\eta_c)^m]^n} \\ &= \phi_2 + \frac{\phi_2 - P_1(\eta_2)}{[1 + (\eta_1/\eta_c)^m]^n}. \end{aligned} \quad (4.5)$$

Therefore  $P_1(\eta_2) = \phi_2$  giving rise to the same problem of point A ( $\eta_1, \phi_1$ ).

- If we choose a point C ( $\eta_3, \phi_3$ ) in region ① but at the left side of  $\eta = \eta_c$ , we obtain

$$\phi_3 = P_1(\eta_3) + \frac{P_2(\eta_3) - P_1(\eta_3)}{[1 + (\eta_3/\eta_c)^m]^n}.$$

It follows that

$$[1 + (\eta_3/\eta_c)^m]^n = \frac{P_2(\eta_3) - P_1(\eta_3)}{\phi_3 - P_1(\eta_3)}. \quad (4.6)$$

However, the LHS of Eq. (4.6) is always positive, but the RHS of (4.6) is negative because  $P_2(\eta_3) < P_1(\eta_3)$  and  $\phi_3 > P_1(\eta_3)$ . Parameters  $m$  and  $n$  cannot be found to resolve this contradiction at ( $\eta_3, \phi_3$ ).

- If we choose a point D ( $\eta_4, \phi_4$ ) in region ① but at the right side of  $\eta = \eta_c$ , we obtain

$$\phi_4 = P_1(\eta_4) + \frac{P_2(\eta_4) - P_1(\eta_4)}{[1 + (\eta_4/\eta_c)^m]^n}.$$

Therefore

$$[1 + (\eta_4/\eta_c)^m]^n = \frac{P_2(\eta_4) - P_1(\eta_4)}{\phi_4 - P_1(\eta_4)}. \quad (4.7)$$

Since  $\phi_4 > P_2(\eta_4)$ , we have  $0 < [1 + (\eta_4/\eta_c)^m]^n < 1$ . In this case, (4.3) can be satisfied only if the exponent  $n$  is negative. However, if  $n$  is negative,  $\phi$  in Eq. (4.3) cannot approach to the two power laws  $P_1$  and  $P_2$  on different sides of  $\eta = \eta_c$ , as expected.

We have shown that the logistic function for power laws  $P_1$  and  $P_2$  has no solution if  $m$  and  $n$  are chosen to match any points in region ① or on the two power laws.

When transition segment is sharp (i.e.  $|m|$  is large and the radius of curvature of the data segment is small), the logistic function (4.3) follows the two power laws closely and the deviation of logistic function from power laws is not even appreciable. In these cases, we do not modify the power laws in data processing because the logistic function can easily satisfy the requirement of fitting error. However, if the radius of curvature of transition segment is large, we want the fitting curve to pass through the data points in a smooth transition. A most convenient way to realize this is to modify the prefactors of the two power laws  $P_1$  and  $P_2$ . Then we can obtain two new power laws  $P'_1$  and  $P'_2$  (see panel (c)). The purpose of the modification is to move all the data points on transition segment out of region ①. In this case, Eq. (4.3) can be processed to fit points on the transition segment. This procedure is not sensitive to small changes in the prefactors of  $P'_1$  and  $P'_2$ . After  $P'_1$  and  $P'_2$  are determined, we choose two points on or nearby the transition segment and substitute into Eq. (4.3) to solve for  $m$  and  $n$  by iterations. In this example,  $P_1, P_2, P'_1$  and  $P'_2$  are  $\phi = 8.41\eta^{0.1429}$ ,  $\phi = 1.89\eta^{0.3726}$ ,  $\phi = 8.76\eta^{0.1429}$  and  $\phi = 2.04\eta^{0.3726}$ , respectively. The threshold value  $\eta_c$  can be determined by letting  $P_1 - P_2 = 0$  and then  $\eta_c = 701.95$ . If we choose points No. 15 and No. 18 (see Table 1) to solve for  $m$  and  $n$ , then we can get  $m = -0.9225$  and  $n = 1.0703$ . Therefore, we have the composite logistic function expressed as

$$\begin{aligned} \phi &= P'_1 + \frac{P'_2 - P'_1}{[1 + (\frac{\eta}{\eta_c})^m]^n} \\ &= 8.76\eta^{0.1429} + \frac{2.04\eta^{0.3726} - 8.76\eta^{0.1429}}{[1 + (\frac{\eta}{701.95})^{-0.9225}]^{1.0703}}. \end{aligned} \quad (4.8)$$

Eq. (4.8) is the rational fraction formula for the data in Table 1 without considering the last 10 points.

The correlation in Eq. (4.8) is shown in panel (d) of Fig. 7, which passes through the data points in segments 1, 2 and 3 perfectly.

Turbulent data suitable for processing as two power law correlations can be found in Figs. 8.5 and 8.8 in the scaling book of Barenblatt [8]. The correlation in Fig. 7 corresponds to 1 in Fig. 8.8 in the Barenblatt book in which the data is described by two broken power laws but no description of the smooth transition between them is given. Keller (2002) introduced a method for constructing a smooth transition between power laws. A differential equation for this problem is proposed and solved. It leads to a power law for

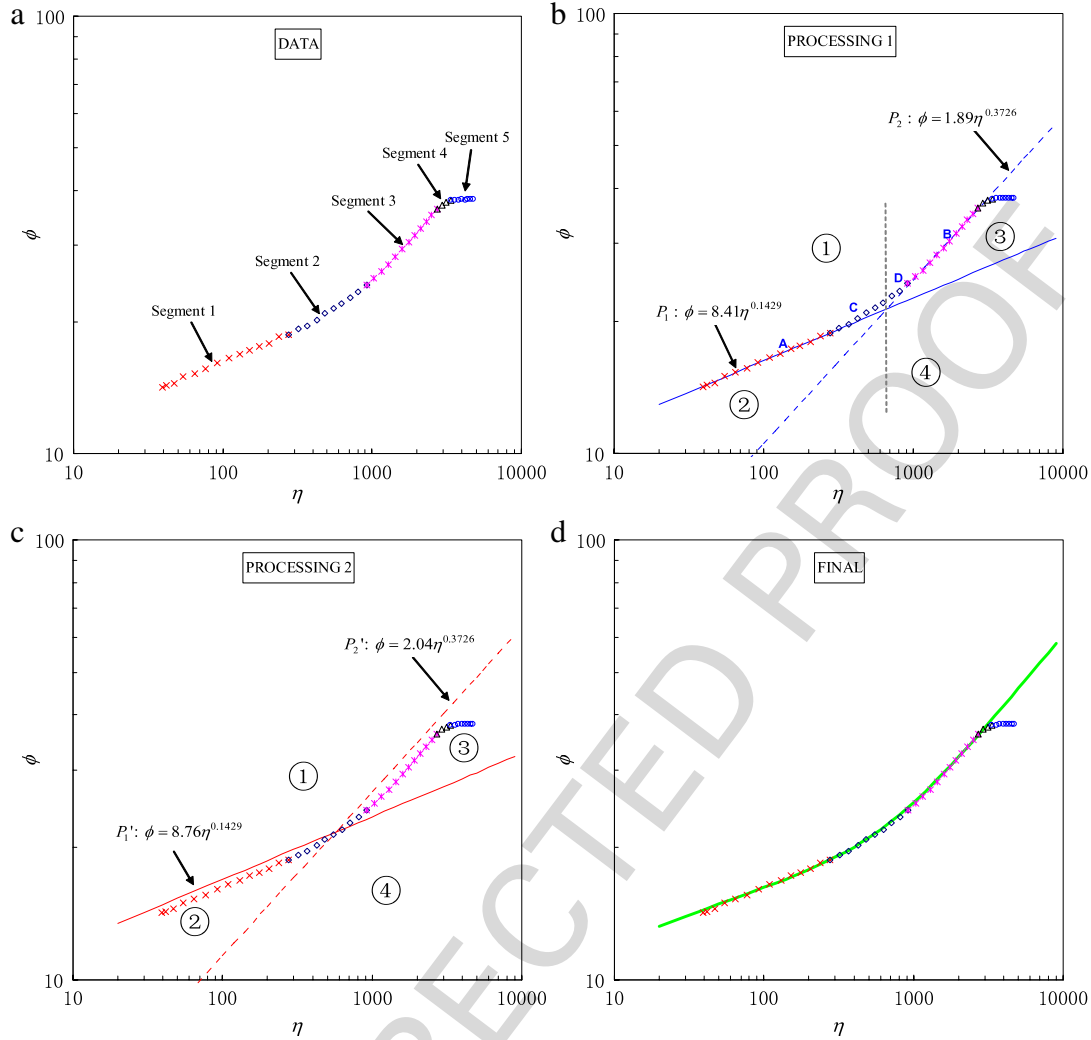


**Fig. 7.** Dimensionless velocity profile vs. dimensionless distance from wall for 30 APG mean flow at  $Re = 19133.02$ . The construction of the logistic dose function as a rational fraction of two power laws is shown in the graphs. The data are from the adverse pressure gradient experiments of Marusic and Perry [15]. The four panels are: (a) the raw data are identified by three power law segments and two transition segments, (b) for segments 1 and 3, two power laws  $P_1$  and  $P_2$  are identified, (c)  $P_1$  and  $P_2$  are modified to  $P_1'$  and  $P_2'$  so that Eq. (4.3) can be processed to fit the points on or nearby the transition segment, (d) the logistic dose function is constructed as a rational fraction of  $P_1'$  and  $P_2'$  after  $m$  and  $n$  are determined (the fitting errors for segments 1, 2 and 3 are less than 1.9% or 0.9% if the first three points are not considered).

the velocity profile followed by a smooth transition to a different power law. Two formulas giving different results are derived; they give different results. Comparisons to data are not given.

## 5. Processing the data of MSZDS [4] for rational fraction correlations between $\lambda$ and $Re$ for laminar, transition and turbulent flow in smooth pipes

More complicated data which requires the use of more than two power laws may require that the exponents as well as the prefactors need to be modified. The selection of these modifications of the power laws depends on the details of data distribution and cannot be specified a priori. The selection of data points for processing even on apparently smooth transition segments are also uncertain in log-log plots where apparently small errors are actually rather large. If improper data points are chosen, the logistic dose function may not have a solution or may give rise to an inaccurate solution. The construction of accurate logistic dose curve solutions is something of an art. A rule of thumb procedure is to estimate the value of  $m$  from the curvature and distribution of data, and then choose only one point from the transition segment to solve for  $n$ . The processing of multi-power law data is carried out in the Appendix, from which we obtain three friction factor correlations  $\lambda$ ,  $\lambda'$  and  $\lambda''$  (see

Eqs. (A.5), (A.7) and (A.9) in Appendix).  $\lambda$  and  $\lambda'$  are generated by connecting four segments of power laws  $\lambda = 64 Re^{-1}$ ,  $\lambda = 4.1 \times 10^{-16} Re^4$ ,  $\lambda = 0.351 Re^{-0.255}$  and  $\lambda = 0.118 Re^{-0.165}$  from different sequences and are in minute agreement with each other.  $\lambda''$  is constructed with the addition of the fifth power law  $\lambda = 19 Re^{-0.82}$  due to the fact that the Oregon data does not agree with the laminar solution  $\lambda = 64 Re^{-1}$  for  $950 < Re < 2900$ . The comparison of  $\lambda''$  with the data of MSZDS [4] is shown in Figs. 8 and 9.

## 6. Roughness

An accurate formula for the full range data of McKeon et al. [4] for pipe flow was derived as a rational fraction of five power laws connected smoothly by the logistic dose function algorithm. The turbulent flow data is represented by a composition of two power laws with errors less than 1% for  $Re < 13 \times 10^6$  but the error increases rapidly thereafter. This rather sudden increase of data can be interpreted as a manifestation of the effect of roughness in an effectively smooth pipe with honed roughness. It is of considerable interest that this critical value was also obtained independently [4] as a lower bound for the manifestation of roughness by studying the error of their best log formula (see Fig. 10).

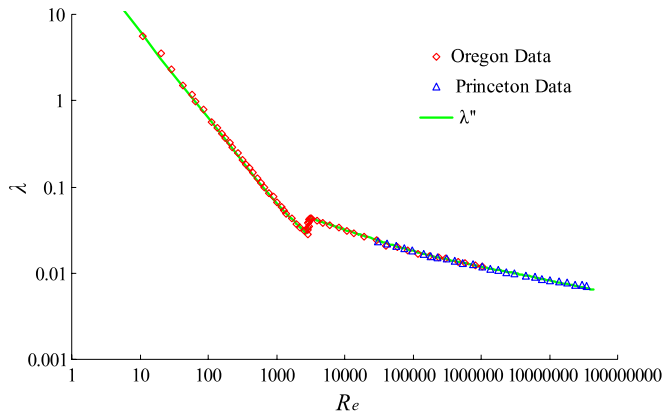


**Fig. 8.** The comparison of logistic fitting curve  $\lambda''$  (see Eq. (A.9) in the Appendix) with the data of MSZDS [4].  $\lambda''$  is a rational fraction of five power laws  $\lambda = 64 Re^{-1}$ ,  $\lambda = 19 Re^{-0.82}$ ,  $\lambda = 4.1 \times 10^{-16} Re^4$ ,  $\lambda = 0.351 Re^{-0.255}$  and  $\lambda = 0.118 Re^{-0.165}$ . The R-square value of  $\lambda''$  is 0.996216 for the full range of Princeton and Oregon data.

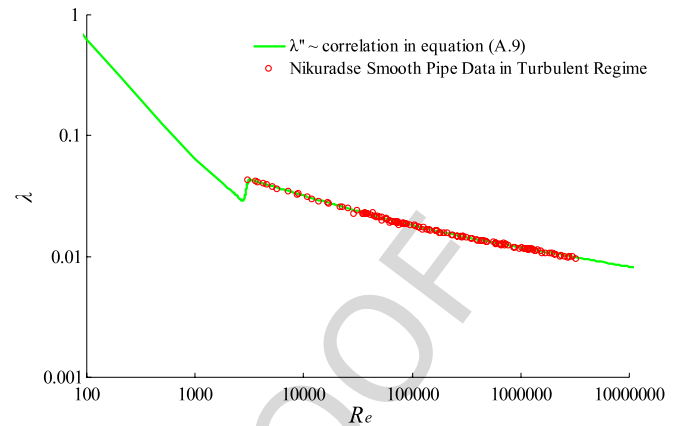


**Fig. 11.** Comparison of Nikuradse's [3] data for turbulent flow in smooth pipes with the correlation  $\lambda''$  (A.9) in the Appendix.

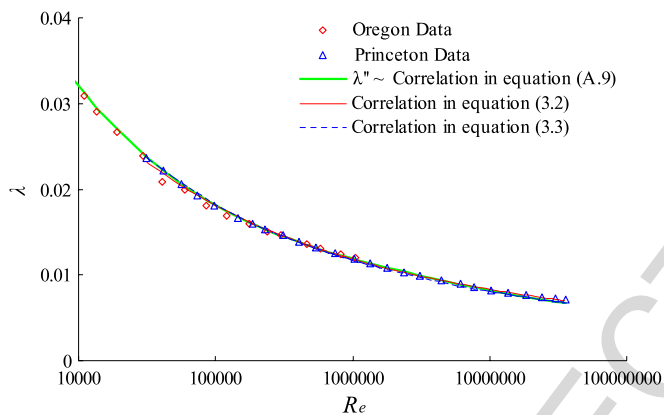


**Fig. 9.** Comparison of MSZDS's data with three fitting curves in Eqs. (3.2), (3.3) and Eq. (A.9) in the Appendix.

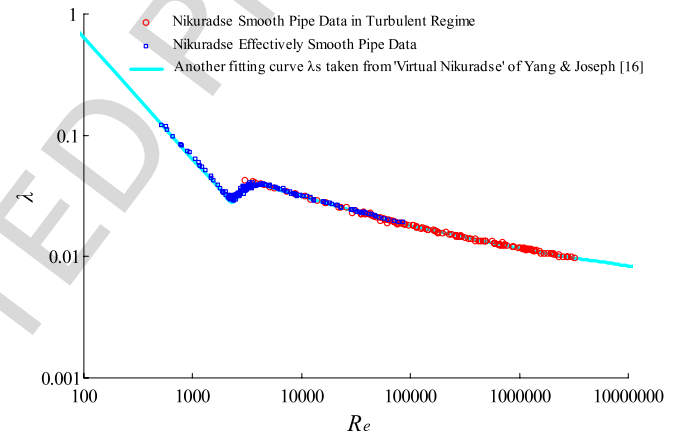


**Fig. 12.** Comparison of Nikuradse's [3,1] data for smooth and effectively smooth pipes with the logistic dose curve  $\lambda_s$  for effectively smooth pipes derived by Yang and Joseph [16].  $\lambda_s$  is constructed from Nikuradse's [1] data by a procedure similar to the one described in this paper;  $\lambda_s$  is a rational fraction of five power laws:  $\lambda = 64/Re$ ,  $\lambda = 0.000083 Re^{0.75}$ ,  $\lambda = 0.3164 Re^{-0.25}$ ,  $\lambda = 0.1537 Re^{-0.185}$  and  $\lambda = 0.0753 Re^{-0.136}$ . The R-square value of  $\lambda_s$  is 0.995444 for the full range of Nikuradse's data for smooth and effectively smooth pipes.

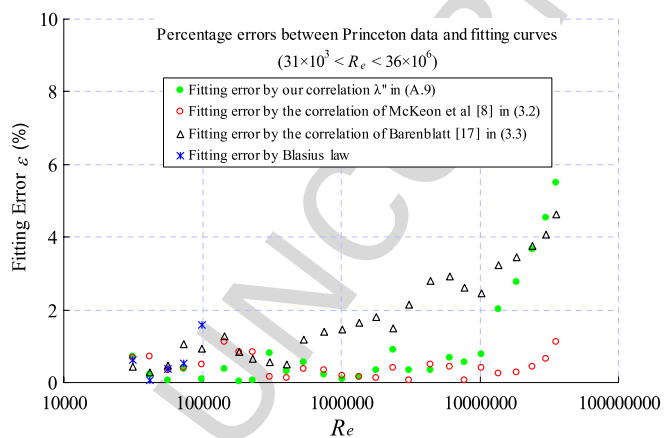


**Fig. 10.** Relative fitting error  $\varepsilon$  vs.  $Re$  between four  $\lambda$ - $Re$  correlations and the Princeton data in turbulent regime ( $31 \times 10^3 < Re < 36 \times 10^6$ ).

We might hope that the quality of our method of logistic dose curve fitting can be improved to arbitrary accuracy, modulo experimental scatter, by choosing more and more branches of power laws and adjusting the sharpness control parameters  $m$  and  $n$  in Eq. (A.1). However, as a practical matter, the implementation of fitting more and more power laws is more and more difficult.

Moreover, in principle, the five-point rule of the logistic dose curve algorithm which is at the center of our fitting method cannot possibly give a perfectly accurate representation of the continuous data connecting power laws (see Fig. 11).

## 7. Friction factor correlation of Nikuradse's data [3,1] for smooth and effectively smooth pipes

We conclude our analysis with a comparison of our rational fraction of power law correlation (A.9) with Nikuradse's data for smooth and effectively smooth pipes. Eq. (A.9) was derived from data of MSZDS [4] but is in satisfactory agreement with the Nikuradse data. The reader will recall that the full range data given by MSZDS is not in good agreement with the full range data [1]. A new full range correlation which coincides with (A.9) in the overlap region is derived in a companion paper by Yang and Joseph [16] on flow in rough pipes is shown Fig. 12.

## 8. Conclusion and discussion

An effectively smooth pipe is one for which the friction factor depends only on the Reynolds number  $\lambda = f(Re)$  and not on roughness. We showed that the bottom envelope of Nikuradse's [1] data

for rough pipes are effectively smooth and in fact coincide with his (1932) data for smooth pipes and with superpipe data presented by McKeon et al. [4] in the interval  $4.2 \times 10^3 < Re < 8.7 \times 10^4$ . The McKeon data is full range over all Reynolds numbers less than  $31 \times 10^6$  combining Oregon data for laminar, transition and turbulent flow with Princeton superpipe data for turbulent flow. The Oregon data for transition and near transition flows of various gases differ strongly with Nikuradse's [1] data for the flow of water. We introduced a new method for processing data. The correlation is given as a rational fraction of rational fractions of power laws which is systematically generated by smoothly connecting linear splines in log–log coordinates with a logistic dose curve algorithm. This kind of correlation seeks the most accurate representation of the data independent of any input from theories arising from the researchers' ideas about the underlying fluid mechanics. As such, these correlations provide an objective metric against which observations and other theoretical correlations may be applied. Our correlation is as accurate, or more accurate, than best log formula of McKeon et al. [4] and incomplete similarity power law formula of Barenblatt et al. [17] in the range of Reynolds numbers in which the correlations overlap. Moreover, our formula is not restricted to certain ranges of Reynolds number but instead applies uniformly to all smooth pipe flow data for which data is available. Our method was applied to data for the mean flow profile in a boundary layer on a flat plate with adverse pressure gradient. We obtained a correlation formula of good accuracy as a rational fraction of two power laws. A highly accurate formula for the full range data of McKeon et al. [4] for pipe flow was derived as a rational fraction of five power laws connected smoothly by the logistic dose function algorithm. The turbulent flow data is represented by a composition of two power laws with errors less than 1% for  $Re < 13.6 \times 10^6$  but the error increases rapidly thereafter. This rather sudden increase of data can be interpreted as a manifestation of the effect of roughness in an effectively smooth pipe with honed roughness. It is of considerable interest, though possibly fortuitous, that this critical value was also obtained independently [4] as a lower bound for the manifestation of roughness by studying the error of their best log formula.

The ideas and methods presented here may be used to correlate complicated engineering data from real and numerical experiments directly into explicit formulas which could never be obtained by mathematical analysis.

## Uncited references

[18].

## Acknowledgements

This work was supported by the NSF/CTS under grant 0076648. We have profited from conversations with G.I. Barenblatt, Ivan Marusic, Beverley McKeon and Alex Smits about topics discussed in this paper. We are indebted to an anonymous referee for calling our attention to the fact that our fitting procedures are not necessarily optimal. Different definitions of optimality will lead to different results; for example, one might look for optimal coefficients which minimize the mean square error.

## Appendix. Fitting procedure for constructing multiple power law correlations between $\lambda$ and $Re$ for smooth pipes

### A.1. Data for the correlation between $\lambda$ and $Re$ for turbulent flow in smooth pipes

Now we will fit data for the correlations between the friction factor  $\lambda$  and the Reynolds number  $Re$ . The modified logistic dose

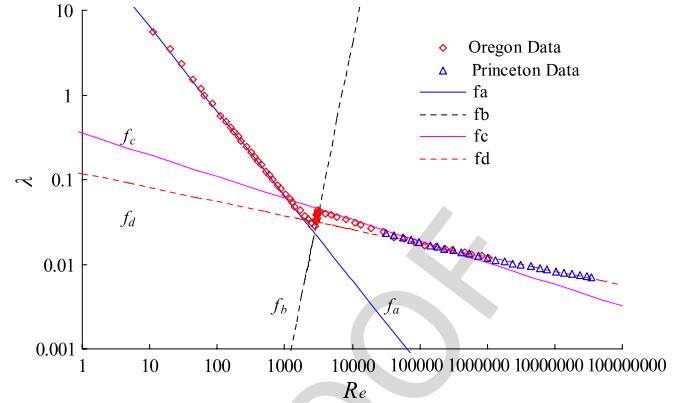


Fig. A.1. Data of MSZDS [4] for friction factors in laminar, transition and turbulent flow in smooth pipes. Four branches of power laws are identified in the plot, and they are  $f_a, f_b, f_c$  and  $f_d$ .

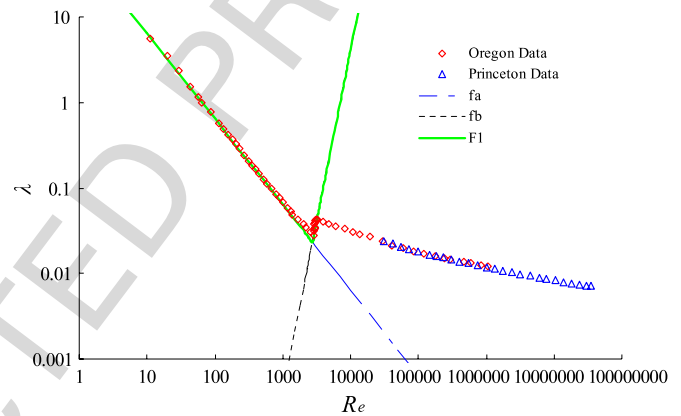


Fig. A.2. The composite logistic dose function  $F_1$  is a rational fraction of two power laws  $f_a$  and  $f_b$  (see Eq. (A.3)).

response curve can be expressed as

$$\lambda = f(Re) = f_L(Re) + \frac{f_R(Re) - f_L(Re)}{[1 + (Re/Re_c)^m]^n}, \quad (\text{A.1})$$

where  $Re_c$  is the critical Reynolds number (i.e. threshold value of Reynolds number),  $f_L$  and  $f_R$  are the two assembly members,  $m$  and  $n$  are constants.

Experimental data of MSZDS [4] for friction factors in turbulent flow in smooth pipes is presented in Fig. 3; the figure shows that the data contains four subsections of straight lines that are distributed in the interval  $(0, 2900)$ ,  $(2900, 3050)$ ,  $(3050, 240\,000)$  and  $(240\,000, +\infty)$ , respectively. The four straight lines represent four branches of power laws in the log–log plot shown in Fig. A.1, and they are

$$f_a = 64 Re^{-1}, \quad f_b = 4.1 \times 10^{-16} Re^4, \quad f_c = 0.351 Re^{-0.255} \\ \text{and } f_d = 0.118 Re^{-0.165}. \quad (\text{A.2})$$

### A.2. Modified logistic dose curve fitting for two power laws

Substituting  $f_L = f_a$  and  $f_R = f_b$  into Eq. (A.1), we obtain a rational fraction for the two subsections  $f_a$  and  $f_b$  in Fig. A.1; identified in Fig. A.2 by a thick solid line in green color, giving rise to the expression

$$F_1 = f_a + \frac{(f_b - f_a)}{[1 + (Re/Re_c)^{-50}]^{0.5}}, \quad (\text{A.3})$$

where the critical Reynolds number  $Re_c$  is 2900.

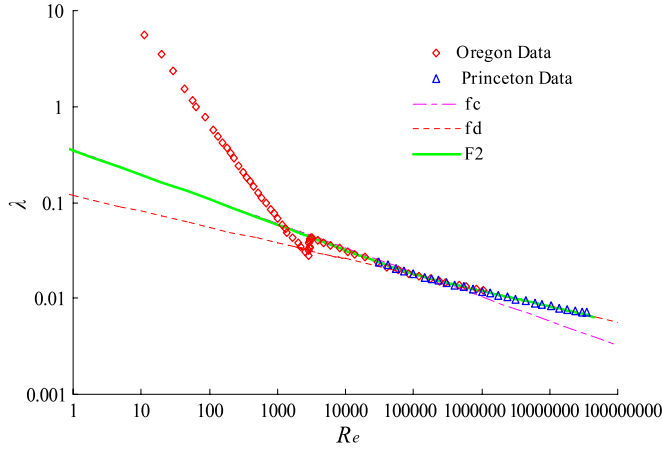


**Fig. A.3.** The composite logistic dose function  $F_2$  is a rational fraction of two power laws  $f_c$  and  $f_d$  (see Eq. (A.4)).

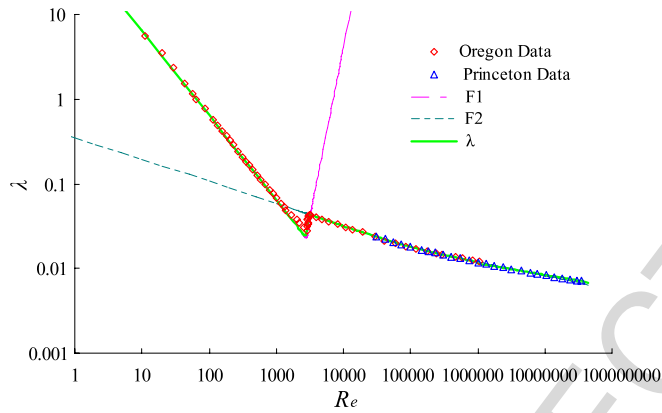


**Fig. A.4.** The composite logistic dose function  $\lambda$  is a rational fraction of two rational fractions  $F_1$  and  $F_2$ , which are logistic dose functions of two power laws (see Eqs. (A.3) and (A.4)).  $\lambda$  is a logistic fitting curve based on four power laws  $f_a, f_b, f_c$  and  $f_d$ .

Similarly, another logistic dose function for the two subsections on the right side is given by

$$F_2 = f_c + \frac{(f_d - f_c)}{\left[1 + (Re/Re'_c)^{-1}\right]^{0.5}}, \quad (\text{A.4})$$

where the critical Reynolds number  $Re'_c$  is 240 000 (see Fig. A.3).

### A.3. Logistic dose curve fitting for two rational fractions of power laws

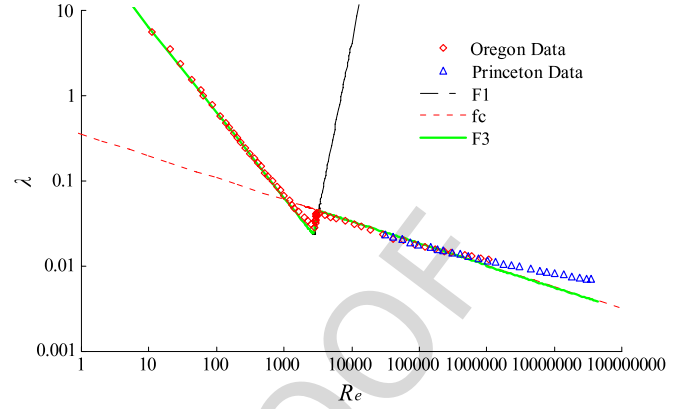
To describe all of the data of MSZDS [4] for friction factors in laminar, transition and turbulent flow in smooth pipes connecting the four branches of power laws, we first replace the two assembly members  $f_L$  and  $f_R$  with  $F_1$  and  $F_2$  which are defined in Appendix A.2. This leads to the following rational fraction of power laws:

$$\lambda = F_1 + \frac{(F_2 - F_1)}{\left[1 + (Re/Re''_c)^{-50}\right]^{0.5}}, \quad (\text{A.5})$$

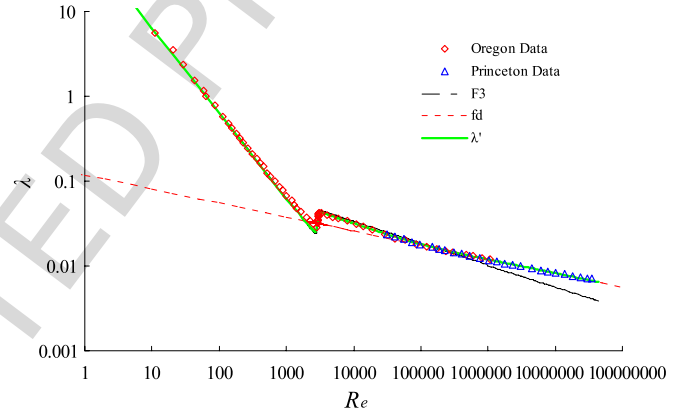
where the critical Reynolds number  $Re''_c$  is 3050 (see Fig. A.4).

Fig. A.4 shows that the fitting curve described in Eq. (A.5) can fit the data of MSZDS [4] nearly perfectly in the full range of Reynolds numbers.

Another procedure for fitting two rational fractions of power laws is to construct a logistic dose function, first for a rational



**Fig. A.5.** The composite logistic dose function  $F_3$  is a rational fraction of two power law rational fraction  $F_1$  and a single power law  $f_c$  (see Eq. (A.6)).



**Fig. A.6.** The composite logistic dose function  $\lambda'$  is a rational fraction of a rational fraction  $F_3$  and a power law  $f_d$ .  $F_3$  is a logistic dose function of three power laws (see Eq. (A.6)).  $\lambda'$  is a logistic fitting curve based on four power laws  $f_a, f_b, f_c$  and  $f_d$ . The R-square value of  $\lambda'$  is 0.996213 for the full range of Princeton and Oregon data.

fraction of three power laws  $f_a, f_b$  and  $f_c$  fit to a fourth power law  $f_d$ . This procedure is exhibited in Figs. A.5 and A.6. Fig. A.5 shows the logistic dose curve fitting of three power laws by replacing  $f_L$  and  $f_R$  in Eq. (A.1) with  $F_1$  and  $f_c$ ; this curve is expressed as

$$F_3 = F_1 + \frac{(f_c - F_1)}{\left[1 + (Re/Re'''_c)^{-50}\right]^{0.5}}, \quad (\text{A.6})$$

where the threshold value of Reynolds number  $Re'''_c = 3050$ .

The logistic dose function  $F_3$  in Eq. (A.6) represents a fitting curve of three power laws. We can combine  $F_3$  with the fourth power law  $f_d$  to obtain the fitting curve for the data of MSZDS [4] for the full range of Reynolds number (see Fig. A.6). The fitting curve is given by

$$\lambda' = F_3 + \frac{(f_d - F_3)}{\left[1 + (Re/Re''''_c)^{-1}\right]^{0.5}}, \quad (\text{A.7})$$

where the threshold value of Reynolds number  $Re''''_c = 240\,000$ .

Figs. A.4 and A.6 show that both procedures lead to fitting curves which agree well with the experimental data. Moreover, the two fitting curves in Eqs. (A.5) and (A.7) are in a good agreement with one another. We have compared the difference between the two curves in Eqs. (A.5) and (A.7), and the results are shown in Fig. A.7 which shows that the relative error between the two curves can be controlled within  $\pm 3\%$ . The large errors mainly occur in the

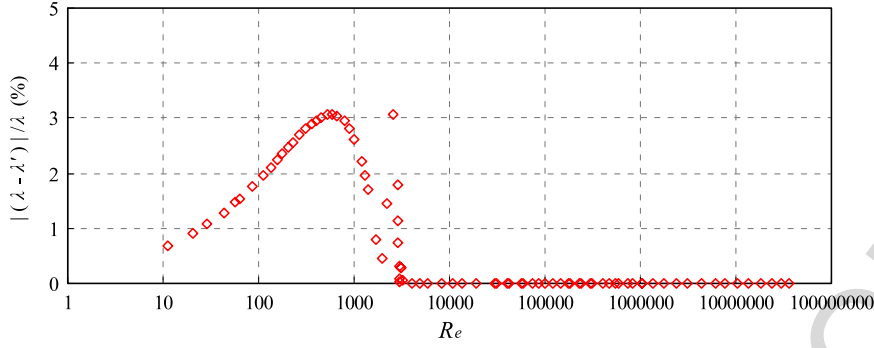


Fig. A.7. Comparison of logistic dose fitting curves  $\lambda$  and  $\lambda'$ .

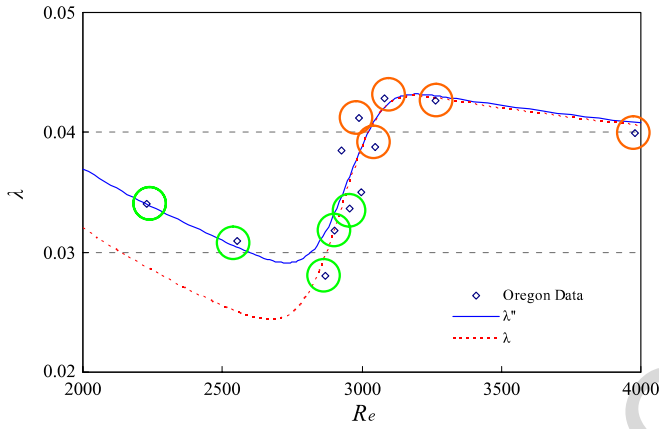


Fig. A.8. The zoom-in view of the modified logistic dose fitting curves  $\lambda'$  and  $\lambda''$  for  $2000 \leq Re \leq 4000$  shows that the logistic dose fitting curves can be improved by choosing more power laws. The two fitting curves  $\lambda'$  and  $\lambda''$  are based on four and five power laws, respectively. The fitting errors on some points cannot be reduced to less than 5%–10% due to the scatter of experimental data. The big circles show the five points which are chosen to fit the data in transition regions.

range of small  $Re$  because Oregon data does not agree well with the theoretical solution  $\lambda = 64/Re$  for laminar flow, which is used in the constructions of correlations (A.5) and (A.7). Another reason is that the power law  $f_b$  is too steep in the log-log plot and logistic close function may not handle it perfectly.

#### A.4. Analysis of fitting error $\varepsilon$

Figs. A.4 and A.6 show that the data does not match the fitting curves perfectly in a small interval around  $Re = 1000$ . The deviation is due to the fact that the data of MSZDS [4] does not match the laminar correlation  $f = 64/Re$ . This deviation of the four power law correlations (A.5) and (A.7) from the experimental data can be reduced by representing the data with five rather than four power laws. The measure of the deviation used here is

$$\varepsilon = \left| \frac{\text{Predicted value by fitting curve} - \text{Observed value in experiment}}{\text{Observed value in experiment}} \right|. \quad (\text{A.8})$$

The five power law construction is carried out as follows: We first split the laminar correlation  $f_a = 64/Re$  into two parts and replace  $f_a$  it with a rational fraction

$$\tilde{f}_a = f_{a1} + \frac{(f_{a2} - f_{a1})}{[1 + (Re/950)^{-10}]^{0.5}}$$

of two power laws  $f_{a1} = f_a = 64/Re$  and  $f_{a2} = 19 Re^{-0.82}$ . Then the fitting curve (A.7) can be updated to

$$\lambda'' = \tilde{F}_3 + \frac{(f_d - \tilde{F}_3)}{[1 + (Re/Re_c''')^{-1}]^{0.5}}, \quad (\text{A.9})$$

where

$$\tilde{F}_3 = \tilde{F}_1 + \frac{(f_c - \tilde{F}_1)}{[1 + (Re/Re_c''')^{-50}]^{0.5}} \quad \text{and}$$

$$\tilde{F}_1 = \tilde{f}_a + \frac{(f_b - \tilde{f}_a)}{[1 + (Re/Re_c)^{-50}]^{0.5}}.$$

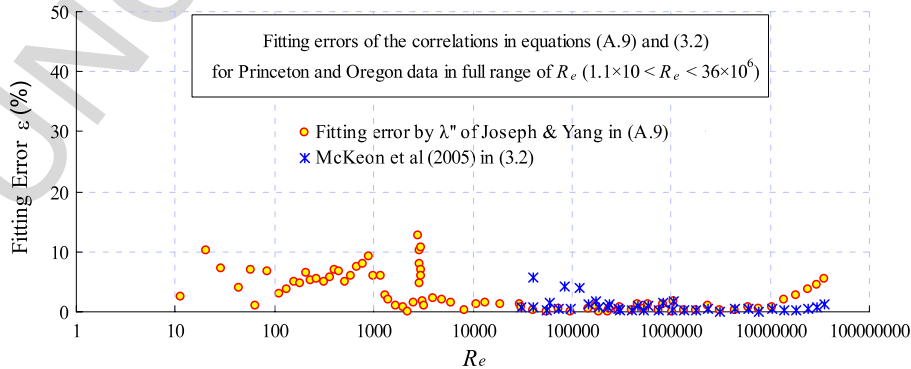


Fig. A.9. Relative fitting error vs.  $Re$  between our logistic dose curve  $\lambda''$  (A.9), the best formula (3.2) of McKeon et al. [6] and the data of MSZDS [4]. McKeon et al. fit their data with an empirical formula based on logarithms rather than powers; their formula fits the data well in a limited range of Reynolds numbers ( $31 \times 10^3 \leq Re \leq 35 \times 10^6$ ) in the turbulent regime. The relative error of their formula (3.2) in representing the data is also shown in this figure. Our Eq. (A.9) applies to the full range of Reynolds numbers given by MSZDS [4] rather than a limited one.

The fitting curve  $\lambda''$  in Eq. (A.9) is shown in Fig. 8. A zoom-in plot of our fitting curve  $\lambda''$  for  $Re$  ranging from 2000 to 4000 is shown in Fig. A.8; the fitting curve  $\lambda''$  passes through the data smoothly, the relative errors of some points, due to scatter, cannot be reduced to less than 5%–10% (see Fig. A.9).

## References

- [1] J. Nikuradse, *Stromungsgesetz in rauhren rohren*, vDI Forschungshefte 361. (English translation: *Laws of flow in rough pipes*). Technical Report, NACA Technical Memorandum 1292. National Advisory Commission for Aeronautics (1950), Washington, DC, 1933.
- [2] G.I. Barenblatt, A.J. Chorin, Scaling laws for fully developed turbulent flow in pipes, *Appl. Mech. Rev.* 50 (7) (1997) 413–429.
- [3] J. Nikuradse, 1932 *Laws of turbulent flow in smooth pipes*, NASA TT F-10: 359, 1966 (English translation).
- [4] B.J. McKeon, C.J. Swanson, M.V. Zaragola, R.J. Donnelly, A.J. Smits, Friction factors for smooth pipe flow, *J. Fluid Mech.* 511 (2004) 41–44.
- [5] B.J. McKeon, High Reynolds number turbulent pipe flow, Ph.D. Thesis, Princeton University, 2003.
- [6] B.J. McKeon, M.V. Zaragola, A.J. Smits, A new friction factor relationship for fully developed pipe flow, *J. Fluid Mech.* 538 (2005) 429–443.
- [7] M.V. Zagarola, Mean flow scaling in turbulent pipe flow, Ph.D. Thesis, Princeton University, 1996.
- [8] G.I. Barenblatt, *Scaling*, Cambridge University Press, 2003.
- [9] N. Balakrishnan, *Handbook of the Logistic Distribution*, Marcel Dekker, New York, 1992.
- [10] N.A. Patankar, D.D. Joseph, J. Wang, R. Barree, M. Conway, M. Asadi, Power law correlations for sediment transport in pressure driven channel flows, *Int. J. Multiphase Flow* 28 (8) (2002) 1269–1292.
- [11] J. Wang, D.D. Joseph, N.A. Patankar, M. Conway, B. Barree, Bi-power law correlations for sedimentation transport in pressure driven channel flows, *Int. J. Multiphase Flow* 29 (3) (2003) 475–494.
- [12] F. Garcia, R. Garcia, J.C. Padrino, C. Matta, J. Trallero, D.D. Joseph, Power law and composite power law friction factor correlations for laminar and turbulent gas–liquid flow in horizontal pipelines, *Int. J. Multiphase Flow* 29 (2003) 1605–1624.
- [13] F. Garcia, R.Z. Garcia, D.D. Joseph, Composite power law holdup correlations in horizontal pipes, *Int. J. Multiphase Flow* 31 (12) (2005) 1276–1303.
- [14] F. Viana, R. Pardo, R. Yáñez, J.L. Trallero, D.D. Joseph, Universal correlation for the rise velocity of long gas bubbles in round pipes, *J. Fluid Mech.* 494 (2003) 379–398.
- [15] Ivan Marušić, A.E. Perry, A wall-wake model for the turbulence structure of boundary layers. Part 2. Further experimental support, *J. Fluid Mech.* 298 (1995) 389–407.
- [16] B.H. Yang, D.D. Joseph, Virtual Nikuradse, *J. Turbulence* 10 (2009) Art. No. N11 pp. 1–28.
- [17] G.I. Barenblatt, A.J. Chorin, V.M. Prostokishin, Scaling laws for fully developed flows in pipes: Discussion of experimental data, *Proc. Natl. Acad. Sci.* 94 (3) (1997) 773–776.
- [18] B.H. Yang, *Topics in the flow of fluids in pipes*, Ph.D. Thesis, University of Minnesota, 2008.